



ACADEMIC
PRESS

Available online at www.sciencedirect.com

SCIENCE @ DIRECT®

Journal of Sound and Vibration 264 (2003) 287–302

JOURNAL OF
SOUND AND
VIBRATION

www.elsevier.com/locate/jsvi

Balancing of machinery with a flexible variable-speed rotor

F. Sève^a, M.A. Andrianoely^a, A. Berlioz^a, R. Dufour^{a,*}, M. Charreyron^b

^a*INSA de Lyon, Laboratoire de Mécanique des Structures, UMR CNRS 5006, Bâtiment Jean d'Alembert 8, Rue des Sciences, Villeurbanne 69621, France*

^b*Tecumseh Europe, Service Etude, 38290 La Verpillère, France*

Received 22 October 2001; accepted 30 May 2002

Abstract

The balancing procedure of machines composed of a flexible rotating part (rotor) and a non-rotating part (stator) mounted on suspensions is presented. The rotating part runs at a variable speed of rotation and is mounted on bearings with variable-speed-dependent characteristics. Assuming that the unbalance masses are relatively well defined, such as in the case of a crank-shaft, the procedure is based on a numerical approach using rotordynamics theory coupled with the Finite Element and Influence Coefficient Methods. An academic rotor/stator model illustrates the procedure. Moreover, the industrial application concerns a refrigerant rotary compressor whose experimental investigation permits validating the model. Assuming that the balancing planes are located on the rotor, it is shown that reducing the vibration level of both rotor and stator requires a balancing procedure using target planes on the rotor and on the stator. In the case of the rotary compressor, this avoids rotor-to-stator rubs and minimizes vibration transmission through pipes and grommets.

© 2002 Elsevier Science Ltd. All rights reserved.

1. Introduction

Rotating machinery is composed of systems capable of transforming or transporting energies. Electric motors, household appliances, internal combustion engines, gas turbine engines, steam turbines, electric generators, industrial compressors and power transmission systems, to name just a few, are the most common rotating machines used to provide electrical, fluid and mechanical energy. Nowadays, due to improvement in performance and reduced energy consumption, this kind of machinery must be capable of variable speeds of rotation to provide variable amounts of energy, depending on requirements. Furthermore, this variable operation avoids start–stop cycles

*Corresponding author. Tel.: +33-472-438202; fax: +33-472-438930.

E-mail address: regis.dufour@insa-lyon.fr (R. Dufour).

and therefore improves reliability. However, designing variable-speed machinery makes it necessary to reduce vibration levels within a wider frequency band. Different kinds of excitation can introduce vibrations to the system. Rotordynamic investigations permit the prediction of the dynamic behaviour whatever the speed of rotation; however, care must be taken to reduce vibration levels caused by unbalance masses.

Generally speaking, the part of a rotating machine that rotates in normal operation is referred to as the rotor (electric rotor, fans, eccentric pump, etc.). At the lowest speed of rotation, the rotor is considered as rigid, but higher speeds of rotation make the rotor flexible and the shape of the centroidal axis changes with speed. The part that does not rotate is referred to as a stator (electric stator, bearings, housing, crankcase, grommets, etc.). Vibrations are transmitted from the rotor to the stator through bearings, fluid, electric fields, etc. Over-pronounced vibration levels occur on the rotor and the stator at certain critical speeds of rotation. This leads to problems such as rotor-to-stator rubs (air gap, fluid film bearings), energy consumed, noise, vibration transmission through connections and suspension, anchorage failure, etc.

Different balancing methods exist to balance flexible rotors. In a recent survey [1], Zhou and Shi reviewed research work on active balancing methods and gave an extensive list of references also containing a passive approach. The modal balancing method and the influence coefficient method (ICM) are the main methods for balancing flexible rotors [2–4]. The former uses the modal parameters and the modal breakdown of the initial unbalance distribution, the rotor being balanced at its critical speeds, step by step, mode after mode [5]. This method is mostly used for balancing high-speed machinery with a number of critical speeds. ICM consists of evaluating the influence of trial masses on the orbits of the planes to be balanced. These planes, called target planes here, can either be chosen on the rotor and/or the stator. The solution of the associated inverse problem gives the ideal correction mass combination that minimizes the vibration levels of the target planes [2,6]. The balancing speeds of the ICM can be either critical speeds or any other speeds.

The contribution of the paper resides in the balancing of a flexible rotor with known initial unbalance masses, mounted on bearings having speed of rotation-dependent characteristics and running with a variable speed of rotation. The objective is to reduce the vibration levels of the rotating and non-rotating parts.

The proposed procedure uses the finite elements method (FEM), rotor dynamics theory and a balancing method to reduce the vibrations of the rotor and the stator. An academic rotor/stator model illustrates the procedure and an industrial application permits comparing the predicted and measured unbalance responses.

2. Proposed balancing procedure

Designing rotating machines requires the prediction of their dynamic behaviour in bending, which depends on unbalance masses. Balancing consists of minimizing the vibration level using correction masses. Initial unbalance masses can be well-defined eccentric masses, such as crankpin, and/or unknown distributed masses, such as those generated by manufacturing faults. The proposed method is concerned with the case where known eccentric masses have a predominant effect related to a residual unbalance mass effect such that a numerical balancing

procedure can be performed. The proposed balancing procedure first consists of a finite element (FE) model based on rotordynamics theory, then in an application of the influence coefficient method (ICM), the latter being explained through an illustrative example of an academic rotor/stators model.

2.1. Balancing

An academic model serves to illustrate the method. It is an extension of the model presented in Ref. [7]. It consists of a shaft–disk–bearing system mounted in two rigid stators mounted on springs. The shaft of length L along the Y -axis is symmetric and the rigid disk is located at $L/3$. Bearings with symmetric damping and stiffness characteristics are located near each end of the shaft. The main characteristics of the rotor and stators are presented in Appendix A.

The axisymmetric sketch of the FE model is shown in Fig. 1. Each node has four degrees of freedom (d.o.f.), two lateral displacements and the two associated rotations:

- The rotor (flexible rotating part) is modelled with 9 two-node beam–shaft elements (from nodes 1 to 10), and 1 one-node disk element situated at node 4.
- The two stators (non-rotating part) are modelled with two-node rigid beam elements with no mass (nodes 11–13 and 14–16, see the grey parts), their mass properties being taken into account by two additional mass elements located at nodes 12 and 15.
- The rotor is linked to the stators with two two-node bearing elements (nodes 2 and 12 belong to the first bearing while nodes 9 and 15 belong to the second bearing).
- The stators are mounted on an external suspension modelled with two additional spring elements located at nodes 12 and 15.

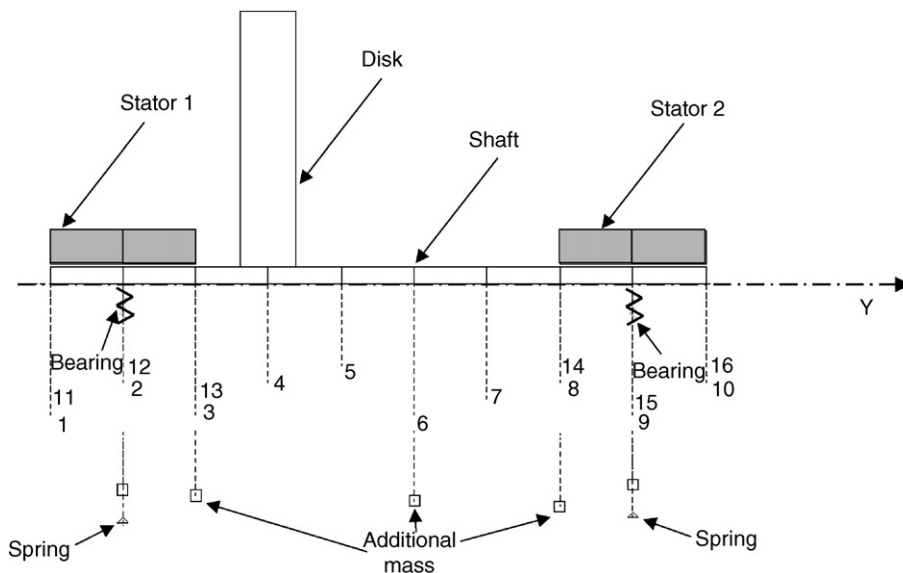


Fig. 1. Academic rotor/stators model.

An initial unbalance mass is located at node 8 and two correction masses are located at nodes 3 and 6.

The assembly yields a 64-equation system that takes the form:

$$(\mathbf{M} + \mathbf{M}_{St})\ddot{\mathbf{X}} + (\mathbf{C}(\Omega) + \mathbf{C}_B + \mathbf{C}_S)\dot{\mathbf{X}} + (\mathbf{K} + \mathbf{K}_B + \mathbf{K}_S)\mathbf{X} = \mathbf{F}(\Omega) \tag{1}$$

with \mathbf{X} being the displacement vector containing all the d.o.f., \mathbf{M} and \mathbf{K} the classical mass and stiffness matrices of the rotor, $\mathbf{C}(\Omega)$ the non-symmetric gyroscopic matrix, \mathbf{C}_B and \mathbf{K}_B the damping and stiffness matrices due to the bearings, \mathbf{M}_{St} the mass matrix of the stators, and \mathbf{C}_S and \mathbf{K}_S the damping and stiffness matrices associated with the suspension. At node i , the component of the force vector $\mathbf{F}(\Omega)$ is created by the unbalance masses $m_i r_i$ positioned at the phase angle ϕ_i as follows:

$$f_x = m_i r_i \Omega^2 \cos(\Omega t + \phi_i), \tag{2}$$

$$f_z = m_i r_i \Omega^2 \sin(\Omega t + \phi_i). \tag{3}$$

This type of model permits the computation of unbalance responses for both the rotor and stator necessary for balancing the entire machine. The unbalance response is predicted using a modal basis and solving a linear system for each value of the speed of rotation Ω .

ICM is chosen in this study because, associated with the least-squares technique, it uses few balancing planes, several speeds of rotation and target planes. The aim of this method is to obtain the correction masses that minimize the amplitude of the target planes' orbits at different balancing speeds (see Fig. 2). ICM can be performed experimentally by measuring the orbits with sensors and fixing trial masses on the balancing planes. However, a numerical investigation can be performed in the case where the eccentric masses are fairly well known and have a predominant effect, in comparison to any initial unbalance distribution due to geometric or material uniformity faults. All that is required is an accurate model of the machine to carry out the necessary successive simulations.

Step one consists in choosing q balancing planes where the correction masses should be located, p target planes where the vibration level has to be minimized and s balancing speeds. If $q = p \times s$, the residual vibration levels can be nil. If $q < p \times s$, the amplitudes cannot be nil but reduced. The efficiency of the balancing depends on the position and number of target planes and also on the number of balancing speeds, which must be known and as representative as possible.

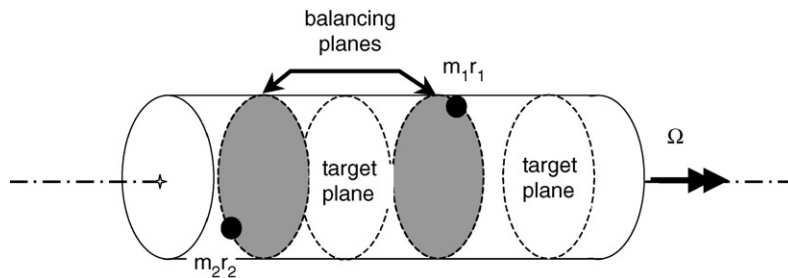


Fig. 2. Balancing and target plane definition.

The following steps consist of predicting the mass unbalance response of the rotor for several additional trial masses, in order to determine the rectangular influence coefficient matrix \mathbf{A} ($p \times s$, q). Then, each coefficient $a_{\ell m}^k$ of \mathbf{A} , where $k = 1, \dots, s$, $\ell = 1, \dots, p$ and $m = 1, \dots, q$, which represents the influence of trial mass m on the vibration level of target plane ℓ at the balancing speed of rotation Ω_k , is calculated according to the formula

$$a_{\ell m}^k = \frac{\bar{\eta}_m^{i+t}(y_\ell, \Omega_k) - \bar{\eta}^i(y_\ell, \Omega_k)}{\bar{U}_m^t} \tag{4}$$

with $\bar{\eta}^i(y_\ell, \Omega_k)$ being the calculated complex amplitude of the initial vibration at speed Ω_k in target plane ℓ having abscissa y_ℓ ; and $\bar{\eta}_m^{i+t}(y_\ell, \Omega_k)$ being the calculated complex amplitude of the vibration at speed Ω_k in the target plane ℓ with a trial correction mass $\bar{U}_m^t = m_m r_m e^{j\theta_m}$ added to the balancing plane m . Parameters m_m , r_m , and θ_m are, respectively the mass, radius of gyration and angular position of trial mass m . The last step is devoted to the calculation of the q correction masses \bar{U}_m^c . In the case where $q < p \times s$, matrix \mathbf{A} is not square and no inversion is possible. The least-squares technique [6] yields the following system:

$$\{\bar{U}_m^c\} = -\{\mathbf{A}^{*T} \mathbf{A}\}^{-1} \mathbf{A}^{*T} \{\bar{\eta}^i(y_\ell, \Omega_k)\}, \tag{5}$$

where \mathbf{A}^* is the conjugate of \mathbf{A} .

2.2. Numerical simulations

Preliminary investigations show that the unbalance response of the academic rotor/stators model, see Fig. 1, exhibits three critical speeds within the [0–7200] r.p.m. range. At the first two critical speeds (600 and 1200 r.p.m.) the rigid rotor deflections have rather cylindrical and conical shapes, respectively, while at the third one (6000 r.p.m.) the rotor deflection is presented in Fig. 3. Usually, two arbitrary balancing planes are chosen, as few balancing planes are accessible on machines. The target planes are chosen depending on the balancing criteria on the rotor or/and on the stator. Balancing speeds are chosen in the operating speed range [1200–7200] r.p.m. which contains the resonance frequencies of the machine, except of course the critical speed of 600 r.p.m.

Three different balancing simulations are presented in what follows to demonstrate the efficiency of the method. The first focuses on the balancing of the rotor only, the second focuses on the balancing of the stator only while the last concerns the entire machine. Table 1 presents the parameters of the three balancings. The correction masses presented in Table 2 are calculated for

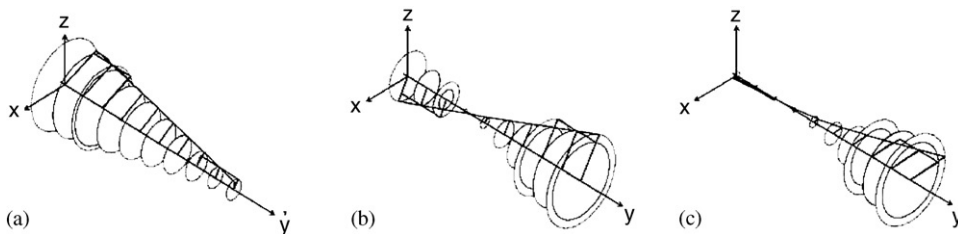


Fig. 3. Academic model. Deflections: (a) ‘cylindrical’ shape at 600 r.p.m., (b) ‘conical’ shape at 1200 r.p.m., and (c) first flexible shape at 6000 r.p.m.

each balancing, by applying the ICM. Displacements at nodes 4, 12 and 15 are presented for each balancing and compared with the unbalanced response of a compressor with no correction masses, Figs. 4–6.

Balancing 1, which concerns the rotor only, obviously improves the dynamic behaviour of the rotor considerably, Fig. 4a, and the vibration level of the stator slightly, Figs. 4b and c. Balancing 2, which concerns the stator only, significantly improves the dynamic behaviour of the stator, except at the highest speeds of rotation where the influence of the unbalance rotor is over-pronounced, Fig. 5. Balancing 3, which concerns the entire machine, improves both rotor and stator motions throughout the [1200–7200] r.p.m. speed range, Fig. 6.

Table 1
Target planes and balancing speeds for the three balancings

	Target plane nodes		Balancing speeds (r.p.m.)
	Rotor	Stators	
Balancing 1	3, 4	—	6000
Balancing 2	—	12, 15	1000
Balancing 3	3, 4	12, 15	1000, 6000

Table 2
Counterweight masses performed with the ICM and for the three balancings

	Plane 1, node 3	Plane 2, node 6
Balancing 1	80 g mm at 5.6°	450 g mm at 179°
Balancing 2	704 g mm at 0°	1670 g mm at 5.6°
Balancing 3	1300 g mm at 2°	1200 g mm at 178°

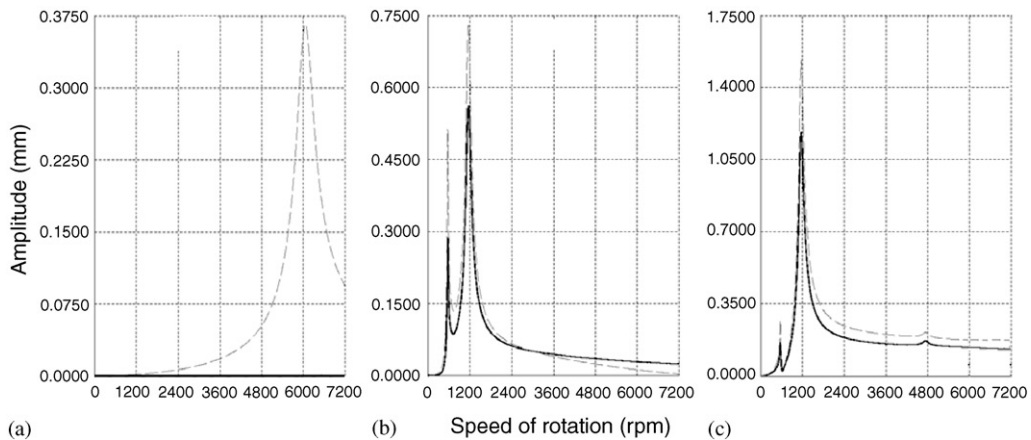


Fig. 4. Academic model. Lateral displacement responses versus speed of rotation with balancing 1 (—), without correction mass (---): (a) rotor, node 4, (b) stator 1, node 12, and (c) stator 2, node 15.

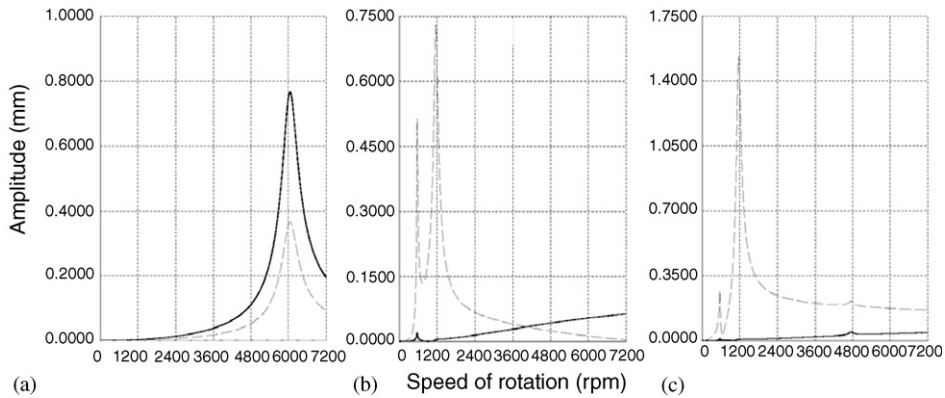


Fig. 5. Academic model. Lateral displacement responses versus speed of rotation with balancing 2 (—), without correction mass (---): (a) rotor, node 4, (b) stator 1, node 12, and (c) stator 2, node 15.

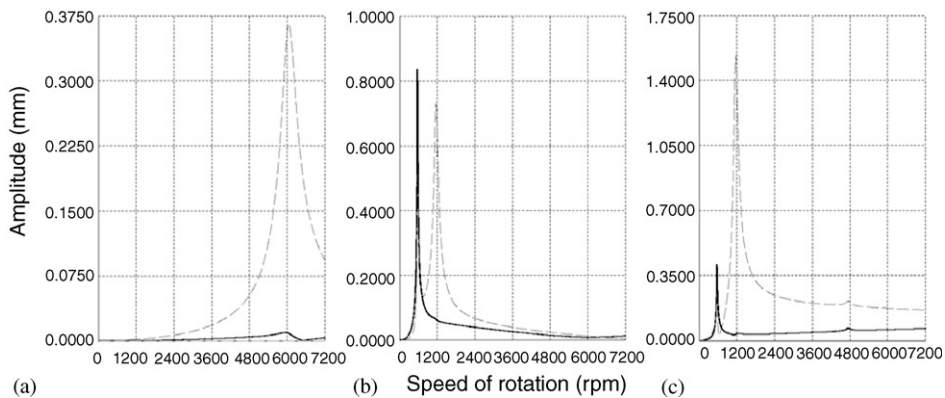


Fig. 6. Academic model. Lateral displacement responses versus speed of rotation with balancing 3 (—), without correction mass (---): (a) rotor, node 4, (b) stator 1, node 12, and (c) stator 2, node 15.

3. Industrial application: balancing of a rotary compressor

3.1. Description

The method presented above is here applied to an industrial machine, in this case a refrigerant rotary compressor. The rotating subassembly, here called a rotor, is composed of an electric rotor, made of steel laminations joined together with aluminium bars, and is fitted onto a crank-shaft made of cast iron. The crankpin of the crank-shaft drives a rolling piston for compressing the refrigerant gas. The non-rotating part, here called a stator, contains an electrical winding press-fitted into the hermetic housing, a two-fluid-film-bearing crankcase containing the pump and welded inside the housing, see Fig. 7. Grommets ensure the vibration insulation of the machine. The rolling piston, crankpin and shoulders of the crank-shaft have fairly well-known eccentric

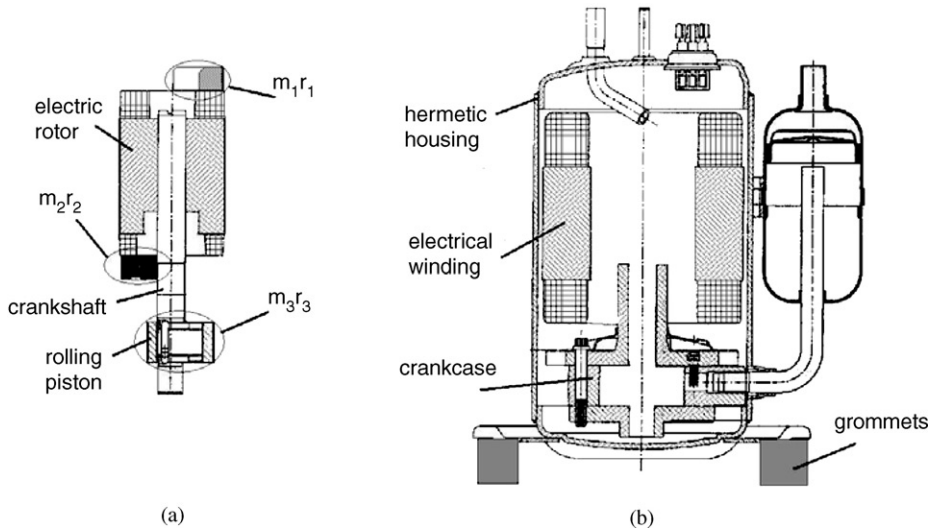


Fig. 7. Rotor (a) and stator (b) of the rotary compressor.

masses. They play a predominant role in the rotordynamics of the machine relative to the residual unbalance masses due to manufacturing faults and design. In order to provide BTU production adaptable to demand, this compressor is capable of a variable speed of rotation within the [1200–7200] r.p.m. range. Therefore, adequate balancing must reduce the vibration level of the rotor and the stator throughout the speed range. FE modelling, experimental validations and application of the method are presented in what follows.

3.2. FE model

In the FE model, the rotor–crank–shaft sub-assembly is considered as a flexural part while the housing–crankcase–stator sub-assembly is assumed to be a rigid body on its grommets [8]. The bearings are modelled with bearing elements whose parameters are variable speed dependent. Side-pull forces between the electric rotor and the stator are also taken into account [9].

The FE modelling follows the same rules as in the academic rotor/stators model, see Section 2.1. The rotor is modelled with beam elements: nodes 1–27. The stator is modelled with rigid beam elements with no mass (nodes from 28 to 44, see the grey parts of Fig. 8), its mass properties being taken into account by an additional mass element located at its centre of inertia (node 44). The coefficients of its mass matrix $\mathbf{M}_{G(44)}$, which has the following expression:

$$\mathbf{M}_{G(44)} = \begin{bmatrix} m & 0 & 0 & 0 \\ & m & 0 & 0 \\ & & I_{XX} & I_{XZ} \\ (sym) & & & I_{ZZ} \end{bmatrix} \tag{6}$$

has been measured with the original oscillatory device described in Ref. [10].

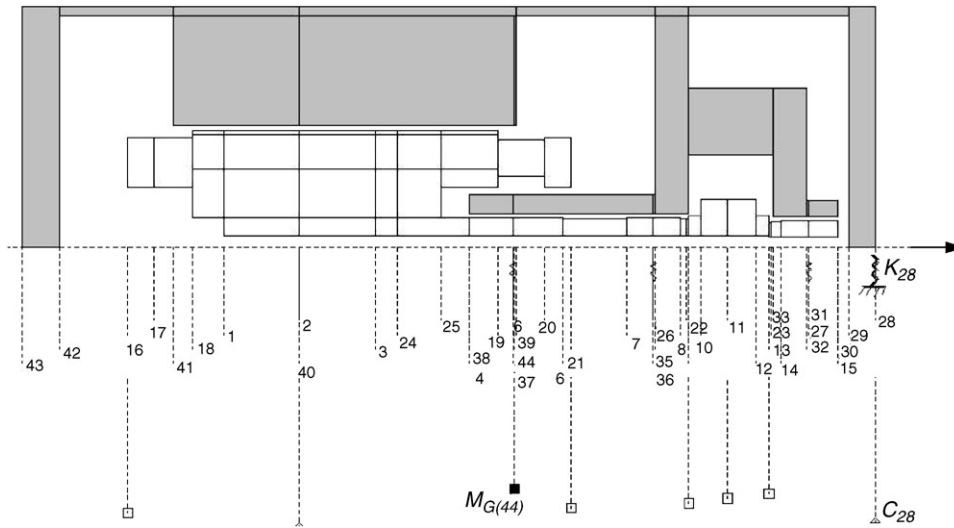


Fig. 8. Finite element model of the compressor.

The rotor is linked to the stator by two-node bearing elements. The main bearing is split into bearing 1 (nodes 5 and 37) and bearing 2 (nodes 26 and 36) and the outboard bearing (bearing 3) located at nodes 27 and 31. The stiffness $K_{xx}, K_{xz}, K_{zz}, K_{zx}$ and damping $C_{xx}, C_{xz}, C_{zz}, C_{zx}$ bearing coefficients, which depend on the speed of rotation, are calculated for six speeds of rotation within the [1200–7200] r.p.m. range.

The support grommets are modelled with an equivalent additional element (assigned to node 28) which has the stiffness and damping matrices:

$$\mathbf{K}_{28} = \begin{bmatrix} 3K_r & 0 & 0 & 0 \\ & 3K_r & 0 & 0 \\ & & \frac{3}{2}K_l \cdot d^2 & 0 \\ (sym) & & & \frac{3}{2}K_l \cdot d^2 \end{bmatrix}, \quad \text{and} \quad \mathbf{C}_{28} = \begin{bmatrix} 3C_r & 0 & 0 & 0 \\ & 3C_r & 0 & 0 \\ & & \frac{3}{2}C_l \cdot d^2 & 0 \\ (sym) & & & \frac{3}{2}C_l \cdot d^2 \end{bmatrix} \quad (7)$$

with K_r, C_r, K_l, C_l being the radial and axial stiffness and damping parameters of a grommet; and d , the distance between the axes of the grommet and of the compressor. The K_r, C_r, K_l, C_l parameters are measured with Forced Response Functions.

Additional masses located at nodes 16 and 21 stand for correction masses m_1 and m_2 while those at nodes 9, 11 and 13 are devoted to eccentric mass m_3 of the pump, with r_1, r_2 and r_3 being the gyration radii, respectively.

In an induction motor, the magnetic field creates side-pull forces on the rotor [9]. It can be modelled by a two-node spring element having a negative stiffness valued at $K_{RS} = 0.5 \times 10^6$ N/m and added between nodes 2 and 40 (see Fig. 2) by way of the matrix

$$\mathbf{K}_2 = \begin{bmatrix} -K_{RS} & 0 \\ 0 & -K_{RS} \end{bmatrix}. \quad (8)$$

The following equations govern the unbalance response of the compressor:

$$(\mathbf{M} + \mathbf{M}_{G(44)})\ddot{\mathbf{X}} + (\mathbf{C}(\Omega) + \mathbf{C}_1(\Omega) + \mathbf{C}_{28})\dot{\mathbf{X}} + (\mathbf{K} + \mathbf{K}_1(\Omega) + \mathbf{K}_2 + \mathbf{K}_{28})\mathbf{X} = \mathbf{F}(\Omega) \quad (9)$$

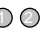

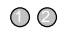
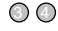
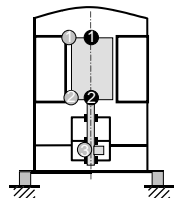
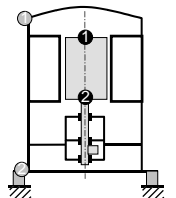
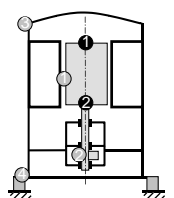


with \mathbf{X} being the displacement vector containing all the d.o.f. of the assembly, \mathbf{M} and \mathbf{K} being the classical mass and stiffness matrices; $\mathbf{C}(\Omega)$, the non-symmetric gyroscopic matrix; $\mathbf{C}_1(\Omega)$ and $\mathbf{K}_1(\Omega)$, the damping and stiffness matrices due to the bearings; $\mathbf{M}_{G(44)}$, the mass matrix of the stator; \mathbf{K}_{28} and \mathbf{C}_{28} , the stiffness and damping matrices associated with the grommets; \mathbf{K}_2 , the anti-stiffness matrix associated with the side-pull forces, and $\mathbf{F}(\Omega)$, the unbalance force vector created by the unbalance masses m_1 , m_2 , and m_3 , as in Eqs. (2) and (3).

3.3. Balancing

The balancing criteria are based on the minimization of the vibration level of the rotor and stator. Industrial requirements make it necessary to keep two existing balancing planes at the top and bottom of the electric rotor [11]. Table 3 lists balancings performed with the proposed method. Four target planes at most are used. They can be located either on the rotor or the stator: balancing 1 focuses on the vibration level of the rotor only, balancing 2 on the vibration level of the stator only and balancing 3 on the vibration level of both rotor and stator. The reference phase (0°) is attributed to the eccentric mass of the pump. Two balancing speeds are used.

The steady state unbalance responses obtained with the three balancings are successively presented and compared with the unbalance responses without correction mass: balancing 1

Table 3
Description of the balancings

	Balancing 1	Balancing 2	Balancing 3
	Three target planes	Two target planes	Two target planes
	on the rotor	on the stator	on the rotor 
			and
			two target planes
			on the stator 
			
Correction mass 	15 g mm at 20°	450 g mm at -4°	Correction masses chosen
Correction mass 	43 g mm at 100°	1319 g mm at 175°	Correction masses chosen

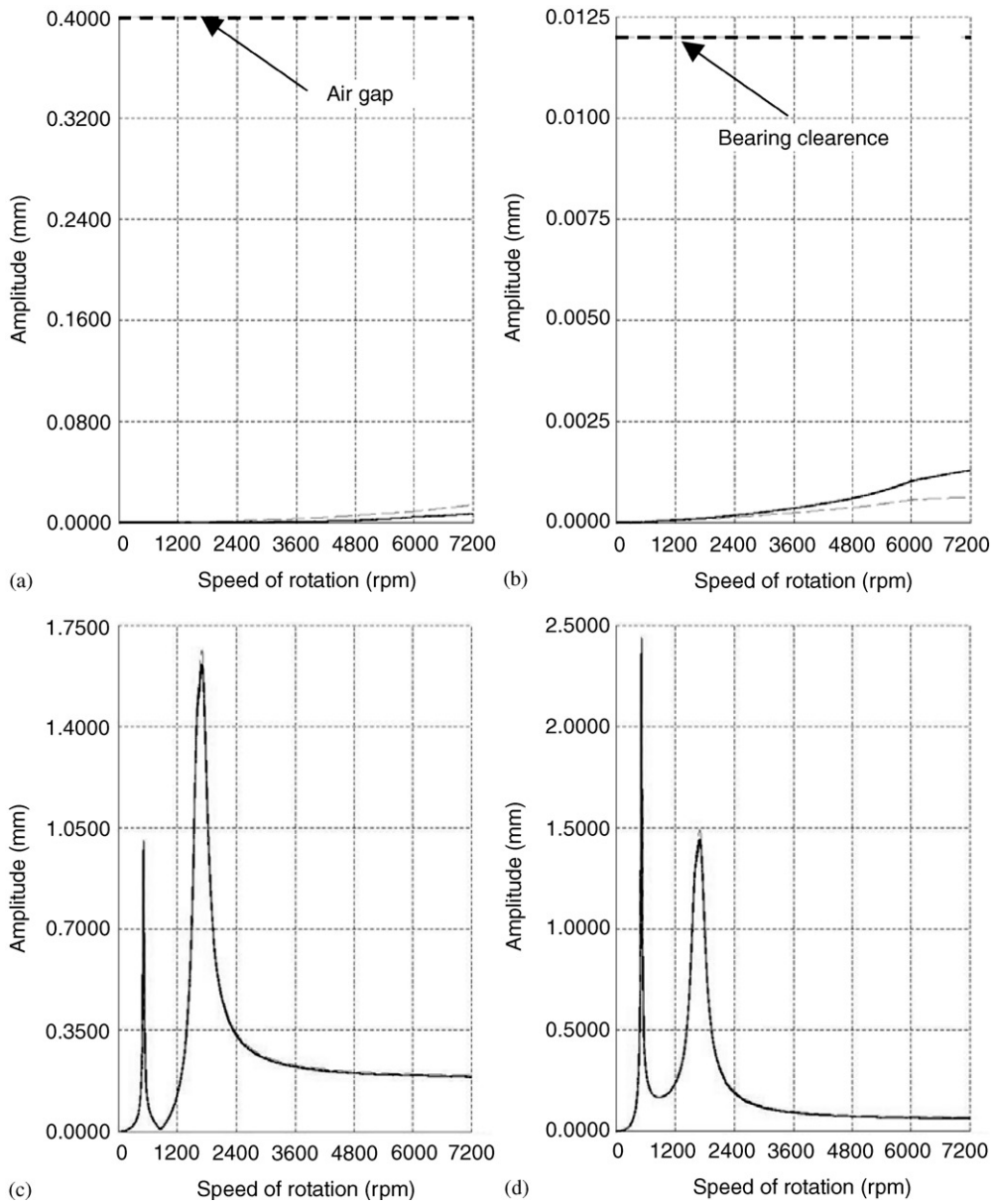


Fig. 9. Industrial application. Lateral displacement responses versus speed of rotation with balancing 1 (—), without correction mass (---): (a) top of the rotor, node 18, (b) main bearing, node 5, (c) bottom of the housing node 28, and (d) top of the housing, node 43.

(Fig. 9), balancing 2 (Fig. 10), and balancing 3 (Fig. 11). Moreover, for each balancing, four lateral displacement responses are presented within the [0–7200] r.p.m. speed range. The first two responses are devoted to the rotor while the other two focus on the stator.

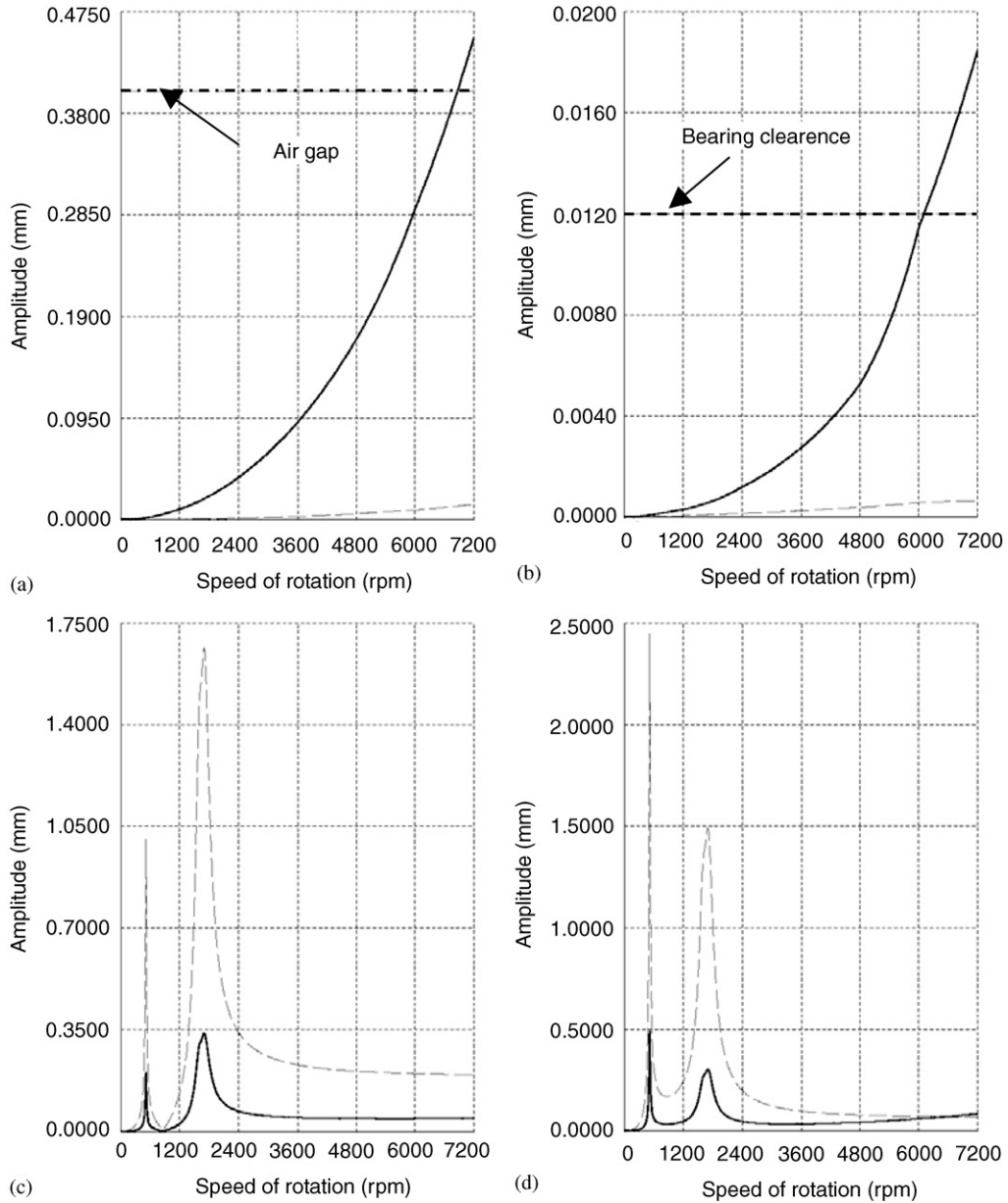


Fig. 10. Industrial application. Lateral displacement responses versus speed of rotation with balancing 2 (—), without correction mass (---): (a) top of the rotor, node 18, (b) main bearing, node 5, (c) bottom of the housing node 28, and (d) top of the housing, node 43.

Balancing 1 concerns the balancing of the rotor. The vibration level of the rotor is far lower than the air gap and the bearing clearance. It is slightly modified, see Figs. 9a and b. The dynamic behaviour of the housing shows two resonance phenomena that correspond to two suspension

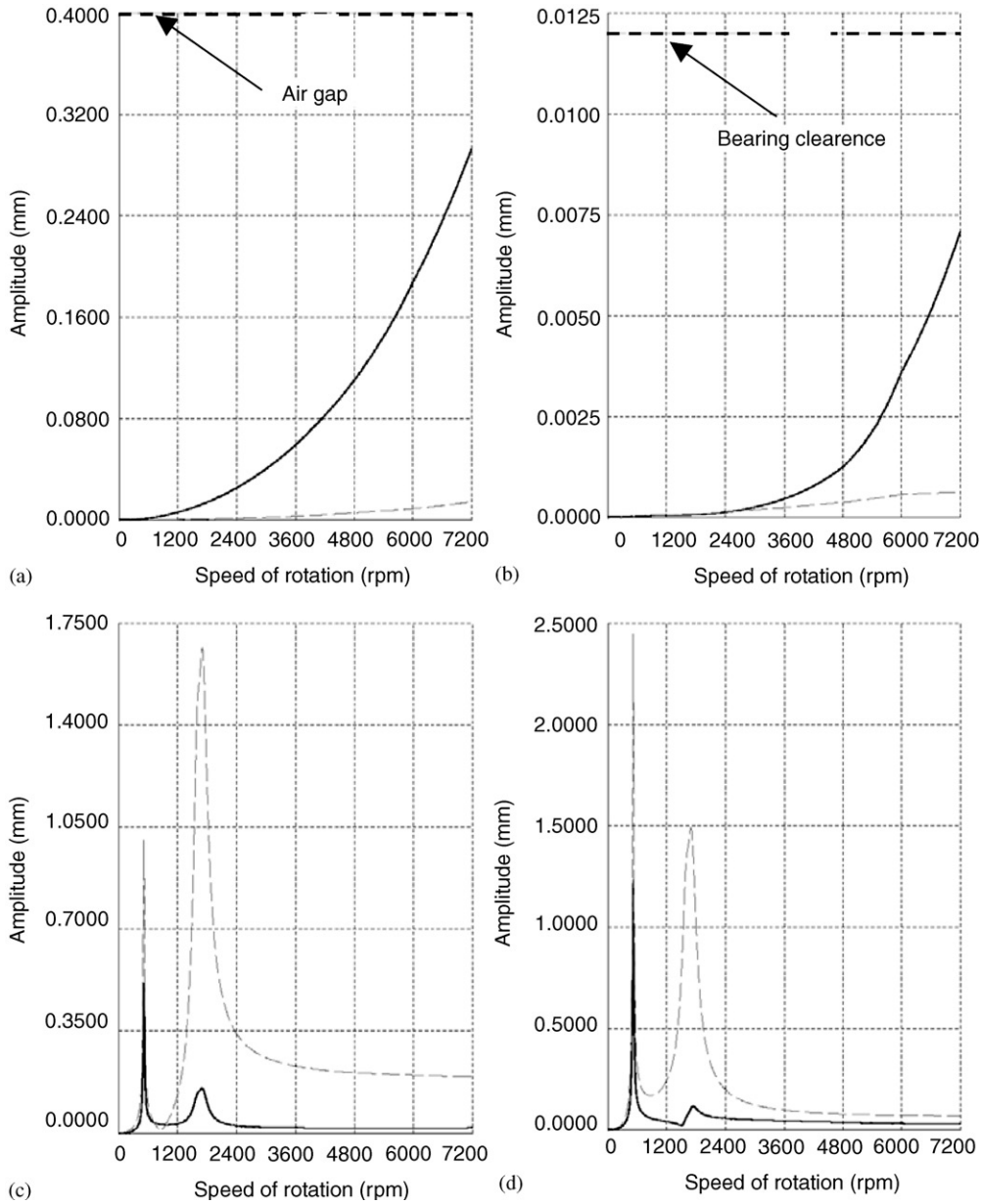


Fig. 11. Industrial application. Lateral displacement responses versus speed of rotation with balancing 3 (—), without correction mass (---): (a) top of the rotor, node 18, (b) main bearing, node 5, (c) bottom of the housing node 28, and (d) top of the housing, node 43.

modes. The balancing has hardly any influence on the housing response, Figs. 9c and d. Balancing 2 concerns the balancing of the stator and significantly improves the housing response, Figs. 10c and d. The vibration level of the rotor is over-pronounced from about 6000 r.p.m.: the air gap, Fig. 10a, and the bearing clearance, Fig. 10b, are reached and the vibration level at the top of the

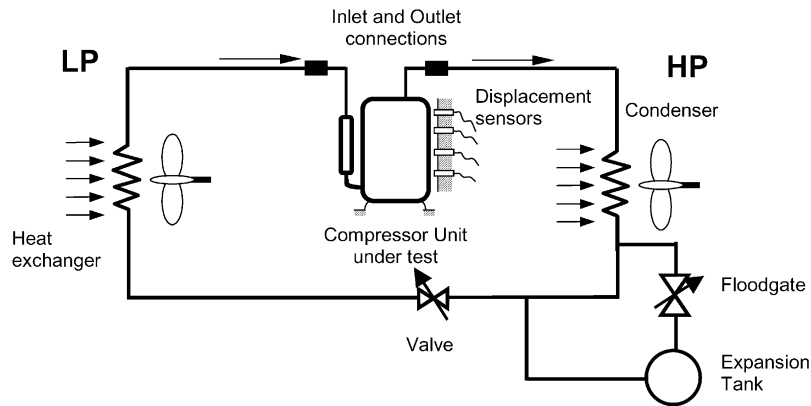


Fig. 12. Bench test.

housing is slightly increased, Fig. 10d. Balancing 3 concerns the balancing of both rotor and stator. The vibration levels of the rotor and the stator are satisfactory in the entire speed range and in particular in the operating [1200–7200] r.p.m. speed range. Balancing 3 is chosen because it permits avoiding rotor-to-stator and bearing-to-crank-shaft rubs, and minimizing the vibration transmission through pipes and grommets.

3.4. Experimental validation

In order to validate the predicted unbalance response, a rotary compressor is incorporated into an air conditioning unit. It consists of a prototype compressor equipped in particular with adjustable correction masses, a thermocouple immersed in an oil bath and mounted by three grommets on a rigid frame. Four orbits distributed along the vertical axis of the housing are measured by proximity probes fixed on a rigid frame, Fig. 12.

The measured and predicted lateral displacements of the housing along its vertical axis are compared throughout the operating speed range in the cases of the three balancings investigated (Fig. 13 shows in particular the results at 4800 r.p.m.). Balancings 1 and 2 make the motion shape of the housing conical while balancing 3 makes it rather cylindrical with a low vibration level. The comparison shows the reliability of the model and permits confirming the previous conclusions drawn from numerical results.

4. Conclusion

Rotating machines are usually composed of a rotating (rotor) and non-rotating parts (stator). It has been shown that in the case where the unbalance masses are well defined, a balancing procedure based on an exclusively numerical approach can be used to reduce the vibration level of the entire machine. Reducing the vibration level of both rotor and stator requires balancing using target planes on the two parts. The influence of the cylinder pressure force, which has not been presented here, has a slight effect relative to the unbalance forces.

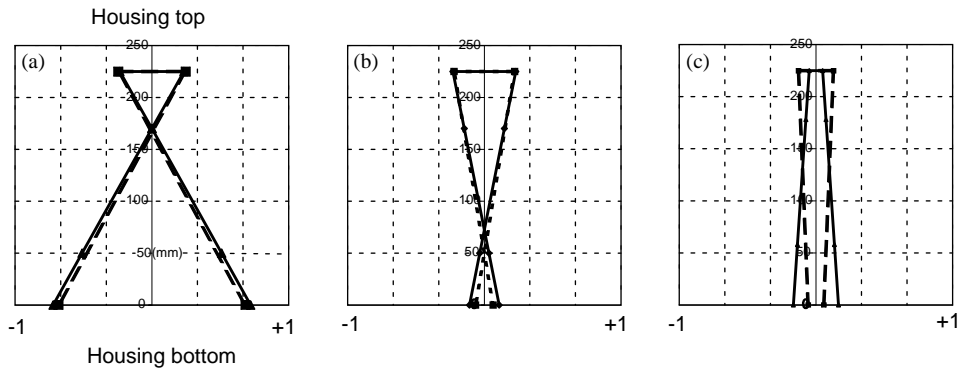


Fig. 13. Maximum dimensionless lateral (---: measured, —: predicted) displacement along the housing: (a) balancing 1, (b) balancing 2, and (c) balancing 3.

In the three balancings tested, the two balancing planes have a fixed location on the rotor, the target planes are first situated on the rotor only, then on the stator only and finally both on the rotor and the stator. The latter balancing was selected because it reduces the vibration level of the rotor and of the stator. Applying this balancing procedure in a variable speed refrigerant rotary compressor permits avoiding rotor-to-stator and bearing-to-crank-shaft rubbing and minimizing vibration transmission through pipes and grommets.

Acknowledgements

The authors are indebted to Tecumseh Europe Co. for its support and permission to publish these works.

Appendix A. Main characteristics of the academic rotor/stators model

Shaft

Length	$L = 0.36$ m
Radius	$R = 0.01$ m
Mass density	$\rho = 7800$ kg/m ³
Young's modulus	$E = 2 \times 10^{11}$ N/m ²
The Poisson ratio	$\nu = 0.3$

Stators

Mass properties

$$M = 4 \text{ kg},$$

$$I_{xx} = I_{zz} = 5 \text{ kg m}^2,$$

$$I_{xz} = I_{zx} = 0.01 \text{ kg m}^2$$

Disk

Inner radius	$R1 = 0.01$ m
Outer radius	$R2 = 0.15$ m

Thickness	$H = 0.03 \text{ m}$
Mass density	$\rho = 7800 \text{ kg/m}^3$
<i>Suspension</i>	
Equivalent stiffnesses	$K_{xx} = K_{zz} = 5 \times 10^4 \text{ N/m}, K_{\theta\theta} = K_{\psi\psi} = 1 \times 10^3 \text{ N m/rad}$
Equivalent damping coefficients	$C_{xx} = C_{zz} = 50 \text{ N s/m}, C_{\theta\theta} = C_{\psi\psi} = 0.1 \text{ N s m/rad}$
<i>Bearing</i>	
Stiffness	$K = 1 \times 10^7 \text{ N/m}$
Damping	$C = 1 \times 10^5 \text{ N s/m}$
<i>Initial unbalance mass (node 8)</i>	
Mass	$M = 0.1 \text{ kg}$
Radius	$D = 0.01 \text{ m}$
Phase	$\phi = 0^\circ$

References

- [1] S. Zhou, S. Shi, Active balancing and vibration control of rotating machinery: a survey, *The Shock and Vibration Digest* 33 (5) (2001) 361–371.
- [2] A.G. Parkinson, The balancing of flexible rotors, *Proceedings of the IUTAM Symposium on Dynamics of Rotors*, Lyngby 1974, pp. 413–435.
- [3] R.E.D. Bishop, G.M.L. Gladwell, The vibration and balancing of an unbalance flexible rotor, *Journal of Mechanical Engineering for Science* 1 (1959) 66–77.
- [4] J.W. Lund, J. Tonnesen, Analyses and experiments on multiplane balancing of a flexible rotor, *American Society of Mechanical Engineers Journal of Engineering for Industry* 94 (1972) 233–242.
- [5] S. Saito, T. Azuma, Balancing of flexible rotors by the complex modal method, *American Society of Mechanical Engineers Journal of Mechanical Design* 105 (1981) 94–105.
- [6] T.P. Goodman, A least squares method for computing balance correction masses, *American Society of Mechanical Engineers Journal of Engineering for Industry* 8 (1964) 273–279.
- [7] M. Lalanne, G. Ferraris, *Rotordynamics Prediction in Engineering*, 2nd Edition, Wiley, New York, 1998.
- [8] F. Sève, A. Berlioz, R. Dufour, M. Charreyron, F. Peyaud, L. Audouy, On the unbalance response of a rotary compressor, *Proceedings of the International Compressor Engineering Conferences of Purdue*, West Lafayette, 2000, pp. 831–838.
- [9] L. Marriot, Finite element calculation of rotor side-pull forces in single-phase induction motors, *Proceedings of the International Compressor Engineering Conferences of Purdue*, West Lafayette, 1994, pp. 729–734.
- [10] K. Gjika, R. Dufour, Rigid body and nonlinear mount identification: application to onboard equipment with hysteretic suspension, *Journal of Vibration and Control* 5 (1999) 75–94.
- [11] F. Sève, A. Berlioz, R. Dufour, M. Charreyron, F. Peyaud, L. Audouy, Balancing of a variable speed rotary compressor: experimental and numerical investigations, *Proceedings of the International Compressor Engineering Conferences of Purdue*, West Lafayette, 2000, pp. 839–446.